Eur. Phys. J. A (2018) **54**: 4
DOI 10.1140/epja/i2018-12451-4

THE EUROPEAN PHYSICAL JOURNAL A

Regular Article – Theoretical Physics

Proton-neutron structure of first and second quadrupole excitations of ^{90}Sr

A.P. Severyukhin[1,2,a], N.N. Arsenyev[1], N. Pietralla[3], and V. Werner[3]

[1] Bogoliubov Laboratory of Theoretical Physics, Joint Institute for Nuclear Research, 141980 Dubna, Moscow region, Russia
[2] Dubna State University, 141982 Dubna, Moscow region, Russia
[3] Institut für Kernphysik, Technische Universität Darmstadt, 64289 Darmstadt, Germany

Received: 26 July 2017 / Revised: 7 December 2017
Published online: 22 January 2018 –
Communicated by F. Gulminelli

Abstract. Starting from the Skyrme interaction f_- together with the density-dependent pairing interaction, we study the g factors for the $2^+_{1,2}$ excitations of ^{88,90}Sr and ^{90,92}Zr. The coupling between one- and two-phonon terms in the wave functions of excited states is taken into account within the finite-rank separable approximation. Using the same set of parameters we describe available experimental data and give the prediction for ^{90}Sr, $g(2^+_2) = +0.03$ in comparison to $+0.31$ in the case of ^{92}Zr.

1 Introduction

Magnetic moments of nuclear quantum states are well known as useful sources of information on their proton-neutron structure. The g factors of the first quadrupole states of even-even nuclei are usually comparable to, though in most cases somewhat smaller than, the collective value Z/A, which would apply to a rotation of a uniformly charged body [1]. Recent experimental studies in nuclei of the $A \approx 90$ mass region have shown that most g factors are close to the Z/A value [2,3]. At the $N = 50$ neutron shell closure the positive large g factors indicate predominant single-particle (SP) proton states, while away from this closed neutron shell both protons and neutrons contribute to the wave functions more equally. However, Zr with 40 protons clearly stands out. Adding neutrons beyond $N = 50$ results in negative g factors (with measured g factor values of $g(2^+_1) = -0.18 \pm 0.02$ for ^{92}Zr and $g(2^+_1) = -0.32 \pm 0.02$ for ^{94}Zr) [4,5]. The neutron configurations dominate in the structure of these 2^+_1 states. A similar structure may be expected for the neighboring Sr isotopes. The main difference is that in Sr the proton $\pi 2p_{1/2}$ orbital is empty, while in Zr it is filled. As a result, the 2^+_1 states have almost equal values of excitation energies, reduced transition probabilities, and g factors [2, 3]. The motivation for this work was to further investigate the g factor evolution for quadrupole collective excitations in ^{90}Sr and ^{92}Zr, in comparison to the isotones ^{88}Sr and ^{90}Zr with $N = 50$ closed neutron shell.

The basic one-phonon quadrupole-collective isovector excitations of the valence shell of heavy nuclei have been predicted as the mixed-symmetry (MS) states in the proton-neutron (pn) version of the interacting boson model (IBM-2) [6]. The pn symmetry of the wave functions is quantified by the bosonic analog of the isospin, termed F spin [7–10]. In particular, there are fully symmetric (FS) states with maximum F spin ($F = F_{max}$) and MS states with $F < F_{max}$. A list of references on that subject is given in ref. [11]. Heyde and Sau described the FS and MS states in the framework of the schematic two-state model (TSM) [12], which has occasionally been used to estimate the properties of quadrupole excitations in the even-even $N = 52$ isotones from ^{92}Zr to ^{100}Cd [5,13]. The TSM consists of a neutron pair and a proton pair, each in a single-j subshell, thus, they are related to d-boson configurations in the IBM-2. Configurations with unperturbed energies are mixed by the residual neutron-proton interaction. The relative phases of proton and neutron amplitudes are opposite in the resulting first and second 2^+ states, *i.e.*,

$$|2^+_{FS}\rangle = \alpha|2^+_\nu\rangle + \beta|2^+_\pi\rangle, \quad (1)$$

$$|2^+_{MS}\rangle = -\beta|2^+_\nu\rangle + \alpha|2^+_\pi\rangle. \quad (2)$$

The amplitudes α and β may reflect two distinct situations: either $\alpha \approx \beta$, leading to well-developed FS and MS states, or $\alpha \neq \beta$. Then, this unbalanced pn content of the wave functions can be interpreted as configurational isospin polarization (CIP) [13], which denotes varying contributions to the 2^+ states by active proton and neutron configurations due to the subshell structure. The CIP effect on structures showing considerable F-spin breaking was first observed in ^{92,94}Zr [5,14–16]. The significantly large $M1$ strength between the $2^+_{1,2}$ states was considered

[a] e-mail: sever@theor.jinr.ru

as the fingerprint of a significant MS character of the 2_2^+ state of ^{92}Zr.

^{92}Zr is lying on the proton $Z = 40$ subshell closure. To consolidate our understanding of structure evolution in this region it is interesting to study the CIP effect on low-energy quadrupole excitations of the next lighter even-even $N = 52$ isotone, ^{90}Sr, theoretically. Our tool is based on the quasiparticle random phase approximation (QRPA) with the Skyrme force f_- [17] in the p-h channel and the density-dependent pairing interaction in a separable approximation for residual interaction. The previously reported [18,19] measured reduction of the $B(E2)$ value of the first 2^+ state of ^{136}Te with respect to ^{132}Te by a factor 1.77 has been reproduced [20] with the Skyrme force f_- in the p-h channel and using the volume zero-range pairing interaction. Based on these calculations we have identified the 2_2^+ state of ^{132}Te as a one-phonon MS state in agreement with experiment. The same calculations indicated the 2_2^+ state of ^{136}Te as a proton-dominated state, corresponding to a MS state with substantial CIP [20]. Recently, available experimental data [18,19] was reanalyzed. For ^{136}Te, the new experimental $B(E2; 0_{gs}^+ \to 2_1^+)$ value of $1810 \pm 150\,\mathrm{e^2fm^4}$ [21] is significantly larger than the previous one of $1220 \pm 180\,\mathrm{e^2fm^4}$, which had at the time misled us to favor the absence of the density-dependent term in the zero-range pairing interaction. The new data leaves the 2_3^+ state of ^{136}Te as the better MS candidate, as predicted in ref. [22]; more experimental data are needed to clarify this point. Since our previous calculation had been optimized to also reproduce the erroneous previous data, it is no surprise that the new $B(E2)$ limits on the 2_2^+ state of ^{136}Te are inconsistent with our previous prediction of it being the MS state [20]. We have done a new calculation with the same f_- Skyrme interaction and only adjusting now the density-dependent term of the pairing interaction to the new data [21]. Our new results are in reasonable agreement with the new data [23].

This paper is organized as follows: in sect. 2, we sketch the method to take into account the coupling between one- and two-phonon terms in the wave functions of excited states. Results of our calculations for properties of the quadrupole-excited states of ^{88,90}Sr and ^{90,92}Zr are given in sect. 3. The effects of the phonon-phonon coupling (PPC) are discussed. Conclusions are drawn in sect. 4.

2 Details of calculations

The method of taking into account the PPC has already been introduced in refs. [20,24,25]. We construct the wave functions from a linear combination of one- and two-phonon configurations as

$$\Psi_\nu(\lambda\mu) = \left(\sum_i R_i(\lambda\nu) Q^+_{\lambda\mu i} + \sum_{\lambda_1 i_1 \lambda_2 i_2} P^{\lambda_1 i_1}_{\lambda_2 i_2}(\lambda\nu) \left[Q^+_{\lambda_1\mu_1 i_1} Q^+_{\lambda_2\mu_2 i_2} \right]_{\lambda\mu} \right) |0\rangle, \tag{3}$$

where λ denotes the total angular momentum and μ is its z-projection in the laboratory system, and with amplitudes $R_i(\lambda\nu)$ and $P^{\lambda_1 i_1}_{\lambda_2 i_2}(\lambda\nu)$. The wave functions of the ground state is the QRPA phonon vacuum $|0\rangle$ and the one-phonon QRPA states given by $Q^+_{\lambda\mu i}|0\rangle$ have energy $\omega_{\lambda i}$. To build the QRPA equations on the basis of HF-BCS quasiparticle states with the residual interactions is a standard procedure [26]. The dimensions of the QRPA matrix grow rapidly with the size of the nucleus. Using the finite rank separable approximation [27] for the residual interactions, the eigenvalues of the QRPA equations can be obtained as the roots of a relatively simple secular equation [28]. It enables us to perform QRPA calculations in very large two-quasiparticle (2QP) spaces. The cut-off of the discretized continuous part of the SP spectra is at the energy of 100 MeV. This is sufficient to exhaust practically all the energy-weighted sum rule. Because of this large configurational space, we do not need effective charges for electric transitions. Nuclear M1 transitions are, however, modified by in-medium effects (meson exchange currents, etc.). Therefore, the $M1$ transition matrix elements are calculated with a spin-gyromagnetic quenching factor $g_s = 0.8$, which improves the overall description of the magnetic properties.

The normalization condition of the wave functions (3) leads to the relation

$$\sum_i R_i^2(\lambda\nu) + 2 \sum_{\lambda_1 i_1 \lambda_2 i_2} \left[P^{\lambda_1 i_1}_{\lambda_2 i_2}(\lambda\nu) \right]^2 \times (1 + K^\lambda(\lambda_1 i_1, \lambda_2 i_2)) = 1, \tag{4}$$

$$K^\lambda(\lambda_1 i_1, \lambda_2 i_2) = (2\lambda_1 + 1)(2\lambda_2 + 1) \times \frac{1}{1 + \delta_{\lambda_1 i_1, \lambda_2 i_2}} \sum_{j_1 j_2 j_3 j_4} (-1)^{j_2 + j_4 + \lambda} \begin{Bmatrix} j_1 & j_2 & \lambda_2 \\ j_4 & j_3 & \lambda_1 \\ \lambda_1 & \lambda_2 & \lambda \end{Bmatrix} \times \left(X^{\lambda_1 i_1}_{j_1 j_4} X^{\lambda_1 i_1}_{j_3 j_4} X^{\lambda_2 i_2}_{j_3 j_2} X^{\lambda_2 i_2}_{j_1 j_2} - Y^{\lambda_1 i_1}_{j_1 j_4} Y^{\lambda_1 i_1}_{j_3 j_4} Y^{\lambda_2 i_2}_{j_3 j_2} Y^{\lambda_2 i_2}_{j_1 j_2} \right).$$

The two-phonon components of the wave functions (3) obey the Pauli principle since we take into account exact commutation relations between the phonon operators, as proposed in ref. [29]. X, Y denote the QRPA amplitudes, the index j is a short notation for the familiar quantum numbers nlj. As an illustration of the Pauli principle corrections, $K^2(2i, 2i)$ values are given in table 1. It is observed that the effect is not negligible. At the same time only minimal corrections occur in the case of ^{90}Zr.

Using the variational principle one obtains a set of linear equations for the amplitudes $R_i(\lambda\nu)$ and $P^{\lambda_1 i_1}_{\lambda_2 i_2}(\lambda\nu)$

$$(\omega_{\lambda i} - E_\nu) R_i(\lambda\nu) + \sum_{\lambda_1 i_1 \lambda_2 i_2} U^{\lambda_1 i_1}_{\lambda_2 i_2}(\lambda i) \times (1 + K^\lambda(\lambda_1 i_1, \lambda_2 i_2)) P^{\lambda_1 i_1}_{\lambda_2 i_2}(\lambda\nu) = 0, \tag{5}$$

$$\sum_i U^{\lambda_1 i_1}_{\lambda_2 i_2}(\lambda i) R_i(\lambda\nu) + 2(\omega_{\lambda_1 i_1} + \omega_{\lambda_2 i_2} + \Delta\omega^\lambda(\lambda_1 i_1, \lambda_2 i_2) - E_\nu) P^{\lambda_1 i_1}_{\lambda_2 i_2}(\lambda\nu) = 0. \tag{6}$$

Table 1. Calculated energies, transition probabilities, g factors, $K \equiv K^2(2i, 2i)$ values and structures of the QRPA quadrupole states of ^{88,90}Sr and ^{90,92}Zr. Phonon amplitude contributions greater than 5% are given. The $M1$ transition matrix elements are calculated without (I) and with the spin-gyromagnetic quenching factor $g_s = 0.8$ (II). Calculated $B(E2)$ values are given in Weisskopf units ($1\,\mathrm{W.u.} = 5.94 \times 10^{-2} A^{4/3}\,\mathrm{e^2fm^4}$).

	λ_i^π	Energy (MeV)	$B(M1; 2_i^+ \to 2_1^+)$ (μ_N^2)		$g(2_i^+)$		$B(E2)\downarrow$ (W.u.)	K	$\{n_1 l_1 j_1, n_2 l_2 j_2\}_\tau$	X	Y	%
			I	II	I	II						
^{88}Sr	2_1^+	1.8			0.71	0.77	8.7	−0.27	$\{2d_{5/2}, 1g_{9/2}\}_\nu$	0.36	0.17	10
									$\{2p_{1/2}, 1f_{5/2}\}_\pi$	0.79	0.12	62
									$\{2p_{1/2}, 2p_{3/2}\}_\pi$	−0.41	−0.09	16
									$\{1f_{5/2}, 1f_{5/2}\}_\pi$	0.36	0.07	6
	2_2^+	2.9	0.12	0.04	0.79	0.83	0.6	−0.29	$\{2p_{1/2}, 2p_{3/2}\}_\pi$	−0.60	0.00	36
									$\{2p_{1/2}, 1f_{5/2}\}_\pi$	−0.56	0.03	31
									$\{1f_{5/2}, 1f_{5/2}\}_\pi$	0.78	0.00	31
^{90}Sr	2_1^+	1.0			−0.09	0.00	9.1	−0.34	$\{2d_{5/2}, 2d_{5/2}\}_\nu$	1.13	0.24	61
									$\{2p_{1/2}, 1f_{5/2}\}_\pi$	0.46	0.20	17
									$\{2p_{1/2}, 2p_{3/2}\}_\pi$	−0.33	−0.16	8
	2_2^+	2.1	0.62	0.55	−0.10	0.04	2.9	−0.19	$\{2d_{5/2}, 2d_{5/2}\}_\nu$	−0.87	0.13	37
									$\{3s_{1/2}, 2d_{5/2}\}_\nu$	0.26	0.05	7
									$\{2p_{1/2}, 1f_{5/2}\}_\pi$	0.66	0.05	43
									$\{2p_{1/2}, 2p_{3/2}\}_\pi$	−0.20	−0.03	5
^{90}Zr	2_1^+	2.5			0.97	0.95	6.8	−0.14	$\{2d_{5/2}, 1g_{9/2}\}_\nu$	−0.37	−0.13	12
									$\{1g_{9/2}, 1g_{9/2}\}_\pi$	0.93	0.08	43
									$\{2p_{1/2}, 1f_{5/2}\}_\pi$	−0.57	−0.06	32
									$\{2p_{1/2}, 2p_{3/2}\}_\pi$	−0.30	−0.04	9
	2_2^+	3.2	0.25	0.13	0.97	0.99	0.01	−0.17	$\{2p_{1/2}, 1f_{5/2}\}_\pi$	0.72	0.01	51
									$\{1g_{9/2}, 1g_{9/2}\}_\pi$	0.98	0.00	48
^{92}Zr	2_1^+	1.3			−0.41	−0.31	3.6	−0.49	$\{2d_{5/2}, 2d_{5/2}\}_\nu$	1.30	0.10	84
									$\{1g_{9/2}, 1g_{9/2}\}_\pi$	0.33	0.12	5
	2_2^+	2.5	0.49	0.38	0.15	0.23	3.7	−0.10	$\{3s_{1/2}, 2d_{5/2}\}_\nu$	−0.49	−0.05	23
									$\{2d_{5/2}, 2d_{5/2}\}_\nu$	−0.57	0.11	15
									$\{1g_{9/2}, 1g_{9/2}\}_\pi$	0.73	0.05	26
									$\{2p_{1/2}, 1f_{5/2}\}_\pi$	−0.46	−0.04	21

For its solution it is required to compute the Hamiltonian matrix elements coupling one- and two-phonon configurations

$$\langle 0|Q_{\lambda i} H \left[Q^+_{\lambda_1 i_1} Q^+_{\lambda_2 i_2}\right]_\lambda |0\rangle = U^{\lambda_1 i_1}_{\lambda_2 i_2}(\lambda i)(1 + K^\lambda(\lambda_1 i_1, \lambda_2 i_2)) \quad (7)$$

and the anharmonic energy shifts of energies of the two-phonon configurations due to the Pauli principle corrections, $\Delta\omega^\lambda(\lambda_1 i_1, \lambda_2 i_2)$ [29,30]. The equations have the same form as the quasiparticle-phonon model (QPM) equations [29,30], but the SP spectrum and the parameters of the residual interaction in Landau-Migdal form are calculated with the chosen Skyrme forces without any further adjustments [24].

The SP spectra around the Fermi level are key ingredients in the microscopic analysis. Among the large number of Skyrme parametrizations, we have selected three, namely, SLy5 [31], f_- [17] and f_+ [17]. The comparably

Table 2. Neutron (ν) and proton (π) single-particle energies (in MeV) near the Fermi energies for ^{90}Zr calculated with Skyrme interactions SLy5, f_- and f_+. The extrapolated "experimental" spectra are taken from ref. [32].

	Expt. [32]	f_-	f_+	SLy5
$\nu 1g_{9/2}$	−12.15(120)	−11.7	−11.8	−11.7
$\nu 2d_{5/2}$	−6.85(70)	−6.5	−6.7	−6.6
$\nu 3s_{1/2}$	−5.63(50)	−4.7	−4.8	−4.8
$\nu 2d_{3/2}$	−4.70(47)	−3.9	−4.0	−4.1
$\pi 1f_{5/2}$	−10.37(110)	−9.8	−10.0	−9.7
$\pi 2p_{3/2}$	−10.11(120)	−10.3	−10.4	−10.3
$\pi 2p_{1/2}$	−6.97(70)	−8.3	−8.3	−8.2
$\pi 1g_{9/2}$	−5.41(54)	−6.6	−6.4	−6.4

Table 3. Energies, transition probabilities, g factors and dominant QRPA components of phonon structures of the low-lying quadrupole states in ^{90}Zr. The PPC calculations are performed without the Pauli principle corrections. Columns A and B give values calculated within the quadrupole-phonon coupling and taking into account the phonon-phonon coupling with the phonons $\lambda^\pi = 2^+, 3^-, 4^+, 5^-$, respectively. Calculated $B(E2)$ values are given in Weisskopf units ($1\,\mathrm{W.u.} = 5.94 \times 10^{-2} A^{4/3}\,\mathrm{e^2fm^4}$). The $M1$ transition matrix elements are calculated with the spin-gyromagnetic quenching factor $g_s = 0.8$.

λ_i^π	Energy (MeV)		Structure		$B(E2)\downarrow$ (W.u.)		$B(E2; 2_i^+ \to 2_1^+)$ (W.u.)		$g(2_i^+)$		$B(M1; 2_i^+ \to 2_1^+)$ (μ_N^2)	
	A	B	A	B	A	B	A	B	A	B	A	B
2_1^+	2.3	2.1	93%$[2_1^+]$	89%$[2_1^+]$	6.5	6.2			0.92	0.88		
2_2^+	3.1	2.8	96%$[2_2^+]$	82%$[2_2^+]$	0.01	0.02	0.2	0.3	1.08	1.00	0.10	0.06

popular set SLy5 has been adjusted to reproduce nuclear matter properties, as well as nuclear charge radii and binding energies of doubly magic nuclei [31]. The SLy5 set is a starting point for the fitting protocol of the series of the three forces, f_-, f_0, and f_+. Thanks to the use of a second density-dependent term in the effective force, this series covers a wide range of isospin splitting of the effective mass (ISEM), defined as $(m_n^* - m_p^*)/m$, with a satisfactory fit to nuclear properties [17]. The forces SLy5 and f_- predict in symmetric matter an effective mass of 0.7, with negative ISEM in neutron-rich systems, namely, -0.182 and -0.284, respectively [17]. The model f_+ leads to an effective mass of 0.7 in symmetric matter and the ISEM equal to $+0.170$ in neutron-rich systems [17]. The selected parametrizations describe correctly the subshell order near the Fermi level of ^{88,90}Sr and ^{90,92}Zr. To see this, the calculated neutron and proton SP energies for the case of ^{90}Zr and the extrapolated "experimental" data [32] are shown in table 2. The ISEM correction is almost unaffected by SP energies, since ^{88,90}Sr and ^{90,92}Zr are not significantly neutron-rich nuclei and, hence, the f_- spectra are very close to those from SLy5. In the present work, we use the force f_- and compare it to the forces SLy5 and f_+ as references that produce similar results. The Landau-Migdal parameters are expressed in terms of the Skyrme force parameters [33]. As proposed in ref. [34] for the forces f_-, f_0, and f_+, we take into account the additional density-dependent term besides the usual density-dependent t_3 term in the expressions for Landau-Migdal parameters.

The pairing correlations are generated by the density-dependent zero-range force

$$V_{pair}(\mathbf{r}_1, \mathbf{r}_2) = V_0 \left(1 - \eta \frac{\rho(r_1)}{\rho_0}\right) \delta(\mathbf{r}_1 - \mathbf{r}_2), \qquad (8)$$

where ρ_0 is the nuclear saturation density; η and V_0 are model parameters. For example, $\eta = 0$ and $\eta = 1$ are the cases of a volume interaction and a surface-peaked interaction, respectively. The strength V_0 is fitted to reproduce the experimental pairing gaps of ^{88,90}Sr and ^{90,92}Zr obtained by the three-point formula [25,28]. The expressions of the Landau-Migdal parameters F_0^{pp}, $F_0^{'pp}$ in terms of the density-dependent force (8) have been obtained self-consistently and can be found in ref. [28]. In order to choose the appropriate value for η, it is very useful to analyze the low-energy two-quasiparticle states, as proposed in ref. [25]. For this purpose, we examine the g factors of the $2_{1,2}^+$ states as a function of the parameter η. In the present work, the parameter $\eta = 0.25$ is fixed to reproduce the experimental g factors of the 2_1^+ states in the studied region of the nuclear chart.

The rank of the set of linear equations (5), (6) is equal to the number of one- and two-phonon configurations. To construct the wave functions (3) of the low-lying 2^+ states up to 4 MeV we use only the 2^+ phonons for computational convenience. This restriction can be justified by the result of recent QPM calculations with large configurational space [35,36], which demonstrate a dominance ($\geq$ 90%) of the 2^+ phonons in the wave functions of the 2_1^+ and 2_2^+ states that are at our focus. To check this, the PPC calculations without the Pauli principle corrections are performed for the case of ^{90}Zr. The present $[2_i^+ \otimes 2_{i'}^+]_{QRPA}$ space (columns A in table 3) is enlarged by the phonon composition with different multipolarities $\lambda^\pi = 2^+, 3^-, 4^+, 5^-$ (columns B in table 3). The obtained results demonstrate the expected unimportance of the two-phonon composition with $\lambda^\pi = 3^-, 4^+, 5^-$ phonons on the $2_{1,2}^+$ properties of ^{90}Zr.

It is worth mentioning that all one- and two-phonon configurations with energies up to $E_{cut} = 8$ MeV are included. The inclusion of high-energy configurations plays a minor role in our calculations. For example, the $E_{cut} = 10$ MeV calculation in the case of ^{90}Sr changes the results for energies and transition probabilities by less than 2%.

3 Results

Inspired by ref. [12] we start out to construct an oversimplified two-state scheme by considering the lowest-energy 2QP-configurations for either neutrons and protons calculated from Skyrme mean-field and the interaction between them. Since their interaction is much smaller than the difference of the corresponding 2QP-energies, the TSM gives the value $\alpha^2 = 0.99$ of both, ^{90}Sr and ^{92}Zr. CIP in the MS and FS states is validated by the amplitudes α and β. For ^{92}Zr the negative $g(2_1^+)$ factor and the large positive $g(2_2^+)$ factor indicate the neutron and proton characters of the respective states. Figures 1 and 2 show energies, g fac-

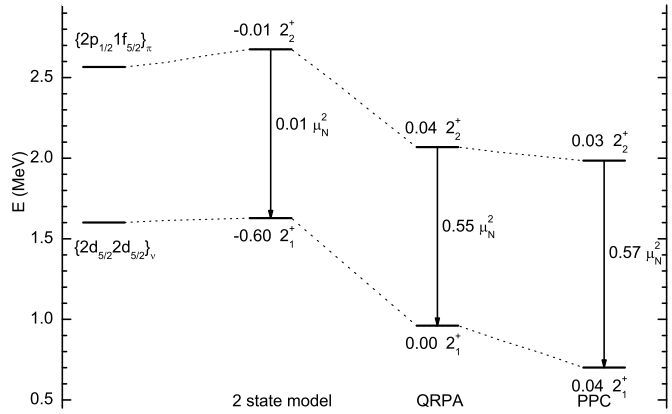

Fig. 1. Energies, g factors and $B(M1)$ values of the $2^+_{1,2}$ states of ^{90}Sr. The columns "2 state model", "QRPA", and "PPC" give values calculated within the two-state model, within the QRPA, and taking into account the PPC, respectively. The $M1$ transition matrix elements are calculated with the spin-gyromagnetic quenching factor $g_s = 0.8$.

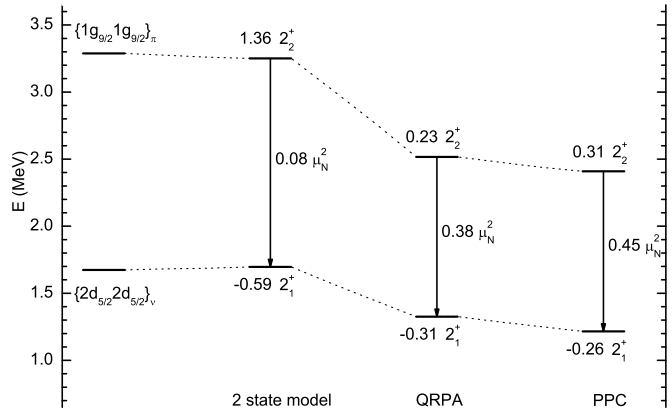

Fig. 2. Same as fig. 1, but for ^{92}Zr.

tors and $B(M1)$ values of the $2^+_{1,2}$ states in ^{90}Sr and ^{92}Zr, respectively. The difference of the proton 2QP configuration in the case of ^{90}Sr results in a $B(M1)$ value of 0.08 μ^2_N in ^{92}Zr, almost eight times larger than that in ^{90}Sr. It is the extension of the variational space to the QRPA phonon configurations that has a strong effect on the g factors and the $B(M1)$ values, see figs. 1 and 2. Structures and $B(E2; 0^+_{gs} \to 2^+_{1,2})$ values of the QRPA states are given in table 1. It is worth pointing out that the TSM cannot allow us to discuss the $E2$ transition, since the 2QP configurations of the giant quadrupole resonance are needed to describe the $B(E2)$ value [40].

Let us now discuss the isotopic dependence of the $[2^+_1]_{QRPA}$ properties near closed shells. The closure of the neutron subshell $1g_{9/2}$ in ^{88}Sr, ^{90}Zr leads to the vanishing of the neutron pairing and as a result energies of the first 2QP poles, $\{2p_{1/2}, 1f_{5/2}\}_\pi$ in ^{88}Sr and $\{1g_{9/2}, 1g_{9/2}\}_\pi$ in ^{90}Zr are larger than the first 2QP energy, $\{2d_{5/2}, 2d_{5/2}\}_\nu$ in ^{90}Sr and ^{92}Zr. This yields that the $[2^+_1]_{QRPA}$ state has collective structure with the domination of the proton 2QP configurations for the case of ^{88}Sr and ^{90}Zr. On the other hand, in ^{92}Zr the leading neutron configuration $\{2d_{5/2}, 2d_{5/2}\}$ gives a contribution of 84% that is almost 1.4 times larger than in ^{90}Sr. The structure peculiarities are reflected in the $g(2^+_1)$ factors and the $B(E2; 0^+_{gs} \to 2^+_1)$ values, as is shown in table 1. The dominant neutron and proton phonon amplitudes X, Y of the 2^+_1 states of ^{90}Sr and ^{92}Zr are in phase. This is an analogy to the FS states of the IBM-2, although we observe the dominance of the neutron configuration $\{2d_{5/2}, 2d_{5/2}\}_\nu$ which can be interpreted as CIP. The $\{2d_{5/2}, 2d_{5/2}\}_\nu$ peculiarity leads to negative $g(2^+_1)$ factors.

We now turn to the structures of the $[2^+_2]_{QRPA}$ states. The proton 2QP-configurations exhaust about 98% in the case of ^{88}Sr and ^{90}Zr. As expected, large positive $g(2^+_2)$ factors are obtained. For the case of ^{90}Sr and ^{92}Zr the main neutron and proton phonon amplitudes of the fairly collective $[2^+_2]_{QRPA}$ state are out of phase. As a consequence, the $B(M1; 2^+_2 \to 2^+_1)$ values are larger than the values in ^{88}Sr and ^{90}Zr. The calculated g factors represent important fingerprints for the pn phonon composition of the $[2^+_2]_{QRPA}$ states of ^{90}Sr and ^{92}Zr. In both nuclei, the main neutron contribution to the g factor comes from the configuration $\{2d_{5/2}, 2d_{5/2}\}_\nu$. This configuration exhausts about 37% and 15% of the wave function normalization of $[2^+_2]_{QRPA}$ state in ^{90}Sr and ^{92}Zr, respectively, causing the strong decrease of the g factor. For ^{92}Zr, the main proton contribution to the g factor comes from the configuration $\{1g_{9/2}, 1g_{9/2}\}_\pi$, which outweighs the neutron contribution and results in a positive $g(2^+_2)$ factor. For ^{90}Sr, this situation changes with the involvement of different proton orbitals due to the breaking of the $Z = 38$ proton subshell closure. This results in a small g factor (table 1). Calculations with the forces SLy5 and f_+ do not change the above conclusion. This QRPA analysis within the one-phonon approximation can help to identify the MS state, but it is only a rough estimate.

We find that the inclusion of the two-phonon configurations further increases the $B(M1)$ values of ^{90}Sr and ^{92}Zr as shown in figs. 1 and 2, respectively. The calculated 2^+ state energies, the largest contributions to the wave function normalization (3), the g factors and the $B(E2)$ and $B(M1)$ values are compared to the experimental data [2–5,15,37–39] in table 4. As one can see in the case of well-known MS state in ^{92}Zr, the agreement of the $B(E2)$ and $B(M1)$ values with the data looks reasonable. The crucial contributions to the wave functions of the $2^+_{1,2}$ states come from the $[2^+_{1,2}]_{QRPA}$ configurations. The dominance of the one-phonon configurations plays the key role to explain the negligible size of the $B(E2; 2^+_2 \to 2^+_1)$ values. For ^{90}Sr and ^{92}Zr, the fragmentation of the $[2^+_1]_{QRPA}$ configuration reduces the $\{2d_{5/2}, 2d_{5/2}\}_\nu$ contribution to the structure of the 2^+_1 state and as a result the $B(M1)$ value and the $g(2^+_1)$ factor are increased. We have examined the amount of the spin contribution to the $M1$ transition strength between the second and first 2^+ states. In fact, we find orbital contributions $\mathcal{M}1(g_s = 0)/\mathcal{M}1(g_s = 0.8)$ of 52% for ^{92}Zr and of 72% for ^{90}Sr to the total $M1$ matrix elements, respectively.

Table 4. Energies, transition probabilities, g factors and dominant QRPA components of phonon structures of the low-lying quadrupole states of ^{88,90}Sr and ^{90,92}Zr. Experimental data are taken from refs. [2–5,15,37–39]. Calculated $B(E2)$ values are given in Weisskopf units ($1\,\mathrm{W.u.} = 5.94 \times 10^{-2} A^{4/3}\,\mathrm{e^2fm^4}$). The $M1$ transition matrix elements are calculated without (I) and with (II) the spin-gyromagnetic quenching factor $g_s = 0.8$.

	λ_i^π	Energy (MeV)		Structure	$B(E2)\downarrow$ (W.u.)		$B(E2; 2_i^+ \to 2_1^+)$ (W.u.)		$g(2_i^+)$			$B(M1; 2_i^+ \to 2_1^+)$ (μ_N^2)		
		Expt.	PPC		Expt.	PPC	Expt.	PPC	Expt.	PPC		Expt.	PPC	
										I	II		I	II
^{88}Sr	2_1^+	1.836	1.7	98%[2_1^+]	7.6(4)	8.6			1.22(11)	0.73	0.77			
	2_2^+	3.218	2.9	98%[2_2^+]	0.10(1)	0.5	0.038(3)	0.04		0.86	0.88	0.073(5)	0.12	0.04
^{90}Sr	2_1^+	0.832	0.7	94%[2_1^+]	8.3(27)	8.9			−0.12(11)	−0.03	0.04			
	2_2^+	1.892	2.0	97%[2_2^+]		2.7		0.5		−0.11	0.03		0.65	0.57
^{90}Zr	2_1^+	2.186	2.4	97%[2_1^+]	5.37(18)	6.6			1.25(21)	0.94	0.93			
	2_2^+	3.308	3.2	98%[2_2^+]	0.44(12)	0.01	2.7(7)	0.1		1.04	1.05	0.088(25)	0.22	0.11
^{92}Zr	2_1^+	0.934	1.2	97%[2_1^+]	$6.4^{+0.6}_{-0.5}$	3.7			−0.18(2)	−0.36	−0.26			
	2_2^+	1.847	2.4	94%[2_2^+]	3.4(4)	3.5	$0.4^{+0.5}_{-0.3}$	0.3	0.76(50)	0.23	0.31	0.37(4)	0.57	0.45

Table 5. QPM calculation: energies, transition probabilities, g factors and dominant QRPA components of phonon structures of the $2^+_{1,2}$ states of ^{92}Zr are taken from [36]. The $M1$ transition matrix elements are calculated with the spin-gyromagnetic quenching factor $g_s = 0.8$.

	2_1^+	2_2^+
Energy (MeV)	1.059	1.983
Structure	93.6%[2_1^+]	92.3%[2_1^+]
$B(E2)\downarrow$ (W.u.)	6.8	3.2
$B(E2; 2_2^+ \to 2_1^+)$ (W.u.)		0.43
$g(2_i^+)$	−0.11	0.72
$B(M1; 2_2^+ \to 2_1^+)$ (μ_N^2)		0.64

It is worth mentioning that the breaking of F-spin symmetry for ^{92}Zr has been confirmed within the QPM before in [35,36]. Table 5 shows the energies, $B(E2)$ and $B(M1)$ values, g factors and dominant QRPA components of phonon structures of the $2^+_{1,2}$ states obtained in the QPM calculation [36]. It was based on the Woods-Saxon potential and the separable two-body Hamiltonian. We should notice that our $2^+_{1,2}$ structures of dominant one-phonon configurations from table 4 are in good agreement with the values from ref. [36] shown in table 5. This probably points to an adequacy of our two-phonon space. Our calculated 2_1^+ energy coincides with the QPM one but our $B(E2)$-value is somewhat smaller likely due to the effective charges $e_p = 1.2$ for protons and $e_n = 0.2$ for neutrons in the QPM [36]. The disagreement for the ratio of pn contributions to the 2_2^+ state is reflected in the factor 1.4 difference of $B(M1; 2_2^+ \to 2_1^+)$ values. A possible source of this discrepancy may be the different SP energy sets in the two approaches.

4 Conclusions

Starting from the Skyrme mean-field calculations we have studied the properties of the low-energy spectrum of 2^+ excitations of ^{90}Sr, ^{92}Zr in comparison to the $N = 50$ isotones ^{88}Sr and ^{90}Zr. Using the Skyrme interaction f_- in connection with the density-dependent pairing interaction, a reasonable description of excitation energies, the $B(E2)$ values and g factors of the first 2^+ states are obtained. For ^{92}Zr, our results indicate that indeed the second 2^+ state is the one-phonon MS state with substantial CIP that was found within the QPM before. The calculated $B(E2)$ and $B(M1)$ values are in reasonable agreement with the experimental data. For ^{90}Sr, we observe a dominance of the neutron configurations in the wave function of the first 2^+ state. The second 2^+ state is identified as a MS state with CIP. The dominant proton configuration is no longer simple single-j subshell recoupling but involves excitation to another subshell. Nevertheless, the $B(M1; 2_2^+ \to 2_1^+)$ value of ^{90}Sr is comparable to the value of ^{92}Zr. For ^{90}Sr, the experimental data of $g(2_1^+)$ is consistent with zero within two standard deviations. Our results give the prediction of $g(2_1^+) = 0.04$, a nearly-vanishing g factor due to the dominance of $\{2d_{5/2}, 2d_{5/2}\}_\nu$ in the 2_1^+ wave function. Further, we predict $g(2_2^+) = 0.03$, which occurs despite the proton dominance in the 2_2^+ wave function, and arises from the more complicated $\{2p_{1/2}, 1f_{5/2}\}_\pi$ and $\{2p_{1/2}, 2p_{3/2}\}_\pi$ configurations as compared to the situation in ^{92}Zr.

For ^{90}Sr, it would be desirable to experimentally confirm the CIP in the 2_2^+ state identified as the one-phonon MS state, to measure its $B(M1; 2_2^+ \to 2_1^+)$ value and the g factor of the 2_2^+ state.

APS and NNA thank the hospitality of Institut für Kernphysik, Technische Universität Darmstadt where a part of this work was done. This work was partly supported by the Heisenberg-Landau program, by the RFBR under Grant No. 16-52-150003 and No. 16-02-00228, by the DFG under grant No. SFB1245.

References

1. A. Bohr, B. Mottelson, *Nuclear Structure*, Vol. **2** (World Scientific, Singapore, 1998).
2. G.J. Kumbartzki, K.-H. Speidel, N. Benczer-Koller, D.A. Torres, Y.Y. Sharon, L. Zamick, S.J.Q. Robinson, P. Maier-Komor, T. Ahn, V. Anagnostatou, Ch. Bernards, M. Elvers, P. Goddard, A. Heinz, G. Ilie, D. Radeck, D. Savran, V. Werner, E. Williams, Phys. Rev. C **85**, 044322 (2012).
3. G.J. Kumbartzki, N. Benczer-Koller, S. Burcher, A. Ratkiewicz, S.L. Rice, Y.Y. Sharon, L. Zamick, K.-H. Speidel, D.A. Torres, K. Sieja, M. McCleskey, A. Cudd, M. Henry, A. Saastamoinen, M. Slater, A. Spiridon, S.Yu. Torilov, V.I. Zherebchevsky, G. Gürdal, S.J.Q. Robinson, S.D. Pain, J.T. Burke, Phys. Rev. C **89**, 064305 (2014).
4. G. Jakob, N. Benczer-Koller, J. Holden, G. Kumbartzki, T.J. Mertzimekis, K.-H. Speidel, R. Ernst, P. Maier-Komor, C.W. Beausang, R. Krücken, Phys. Lett. B **494**, 187 (2000).
5. V. Werner, N. Benczer-Koller, G. Kumbartzki, J.D. Holt, P. Boutachkov, E. Stefanova, M. Perry, N. Pietralla, H. Ai, K. Aleksandrova, G. Anderson, R.B. Cakirli, R.J. Casperson, R.F. Casten, M. Chamberlain, C. Copos, B. Darakchieva, S. Eckel, M. Evtimova, C.R. Fitzpatrick, A.B. Garnsworthy, G. Gürdal, A. Heinz, D. Kovacheva, C. Lambie-Hanson, X. Liang, P. Manchev, E.A. McCutchan, D.A. Meyer, J. Qian, A. Schmidt, N.J. Thompson, E. Williams, R. Winkler, Phys. Rev. C **78**, 031301(R) (2008).
6. F. Iachello, A. Arima, *The Interacting Boson Model* (Cambridge University Press, Cambridge, 1987).
7. A. Arima, T. Otsuka, F. Iachello, I. Talmi, Phys. Lett. B **66**, 205 (1977).
8. T. Otsuka, A. Arima, F. Iachello, Nucl. Phys. A **309**, 1 (1978).
9. F. Iachello, Phys. Rev. Lett. **53**, 1427 (1984).
10. N. Pietralla, C. Fransen, D. Belic, P. von Brentano, C. Frießner, U. Kneissl, A. Linnemann, A. Nord, H.H. Pitz, T. Otsuka, I. Schneider, V. Werner, I. Wiedenhöver, Phys. Rev. Lett. **83**, 1303 (1999).
11. N. Pietralla, P. von Brentano, A.F. Lisetskiy, Prog. Part. Nucl. Phys. **60**, 225 (2008).
12. K. Heyde, J. Sau, Phys. Rev. C **33**, 1050 (1986).
13. J.D. Holt, N. Pietralla, J.W. Holt, T.T.S. Kuo, G. Rainovski, Phys. Rev. C **76**, 034325 (2007).
14. V. Werner, D. Belic, P. von Brentano, C. Fransen, A. Gade, H. von Garrel, J. Jolie, U. Kneissl, C. Kohstall, A. Linnemann, A.F. Lisetskiy, N. Pietralla, H.H. Pitz, M. Scheck, K.-H. Speidel, F. Stedil, S.W. Yates, Phys. Lett. B **550**, 140 (2002).
15. C. Fransen, V. Werner, D. Bandyopadhyay, N. Boukharouba, S.R. Lesher, M.T. McEllistrem, J. Jolie, N. Pietralla, P. von Brentano, S.W. Yates, Phys. Rev. C **71**, 054304 (2005).
16. E. Elhami, J.N. Orce, S. Mukhopadhyay, S.N. Choudry, M. Scheck, M.T. McEllistrem, S.W. Yates, Phys. Rev. C **75**, 011301(R) (2007) **88**, 029902(E) (2013).
17. T. Lesinski, K. Bennaceur, T. Duguet, J. Meyer, Phys. Rev. C **74**, 044315 (2006).
18. D.C. Radford, C. Baktash, J.R. Beene, B. Fuentes, A. Galindo-Uribarri, C.J. Gross, P.A. Hausladen, T.A. Lewis, P.E. Mueller, E. Padilla, D. Shapira, D.W. Stracener, C.-H. Yu, C.J. Barton, M.A. Caprio, L. Coraggio, A. Covello, A. Gargano, D.J. Hartley, N.V. Zamfir, Phys. Rev. Lett. **88**, 222501 (2002).
19. M. Danchev, G. Rainovski, N. Pietralla, A. Gargano, A. Covello, C. Baktash, J.R. Beene, C.R. Bingham, A. Galindo-Uribarri, K.A. Gladnishki, C.J. Gross, V.Yu. Ponomarev, D.C. Radford, L.L. Riedinger, M. Scheck, A.E. Stuchbery, J. Wambach, C.-H. Yu, N.V. Zamfir, Phys. Rev. C **84**, 061306(R) (2011).
20. A.P. Severyukhin, N.N. Arsenyev, N. Pietralla, V. Werner, Phys. Rev. C **90**, 011306(R) (2014).
21. J.M. Allmond, A.E. Stuchbery, C. Baktash, A. Gargano, A. Galindo-Uribarri, D.C. Radford, C.R. Bingham, B.A. Brown, L. Coraggio, A. Covello, M. Danchev, C.J. Gross, P.A. Hausladen, N. Itaco, K. Lagergren, E. Padilla-Rodal, J. Pavan, M.A. Riley, N.J. Stone, D.W. Stracener, R.L. Varner, C.-H. Yu, Phys. Rev. Lett. **118**, 092503 (2017).
22. A. Covello, L. Coraggio, A. Gargano, N. Itaco, Prog. Part. Nucl. Phys. **59**, 401 (2007).
23. A.P. Severyukhin, N.N. Arsenyev, N. Pietralla, V. Werner, in preparation.
24. A.P. Severyukhin, V.V. Voronov, Nguyen Van Giai, Eur. Phys. J. A **22**, 397 (2004).
25. A.P. Severyukhin, N.N. Arsenyev, N. Pietralla, Phys. Rev. C **86**, 024311 (2012).
26. J. Terasaki, J. Engel, M. Bender, J. Dobaczewski, W. Nazarewicz, M. Stoitsov, Phys. Rev. C **71**, 034310 (2005).
27. Nguyen Van Giai, Ch. Stoyanov, V.V. Voronov, Phys. Rev. C **57**, 1204 (1998).
28. A.P. Severyukhin, V.V. Voronov, Nguyen Van Giai, Phys. Rev. C **77**, 024322 (2008).
29. V.G. Soloviev, *Theory of Atomic Nuclei: Quasiparticles and Phonons* (Institute of Physics, Bristol and Philadelphia, 1992).
30. V.V. Voronov, D. Karadjov, F. Catara, A.P. Severyukhin, Phys. Part. Nucl. **31**, 452 (2000).
31. E. Chabanat, P. Bonche, P. Haensel, J. Meyer, R. Schaeffer, Nucl. Phys. A **635**, 231 (1998).
32. O.V. Bespalova, I.N. Boboshin, V.V. Varlamov, T.A. Ermakova, B.S. Ishkhanov, E.A. Romanovsky, T.I. Spasskaya, T.P. Timokhina, Phys. At. Nucl. **69**, 796 (2006).
33. Nguyen Van Giai, H. Sagawa, Phys. Lett. B **106**, 379 (1981).
34. A.P. Severyukhin, J. Margueron, I.N. Borzov, Nguyen Van Giai, Phys. Rev. C **91**, 034322 (2015).
35. N. Lo Iudice, Ch. Stoyanov, Phys. Rev. C **69**, 044312 (2004).
36. N. Lo Iudice, Ch. Stoyanov, Phys. Rev. C **73**, 037305 (2006).
37. E.A. McCutchan, A.A. Sonzogni, Nucl. Data Sheets **115**, 135 (2014).
38. H. Mach, F.K. Wohn, G. Molnár, K. Sistemich, J.C. Hill, M. Moszyński, R.L. Gill, W. Krips, D.S. Brenner, Nucl. Phys. A **523**, 197 (1991).

39. P.E. Garrett, W. Younes, J.A. Becker, L.A. Bernstein, E.M. Baum, D.P. DiPrete, R.A. Gatenby, E.L. Johnson, C.A. McGrath, S.W. Yates, M. Devlin, N. Fotiades, R.O. Nelson, B.A. Brown, Phys. Rev. C **68**, 024312 (2003).
40. C. Walz, H. Fujita, A. Krugmann, P. von Neumann-Cosel, N. Pietralla, V.Yu. Ponomarev, A. Scheikh-Obeid, J. Wambach, Phys. Rev. Lett. **106**, 062501 (2011).